

PACS 42.55.Lt

Polarization unstabilities in a quasi-isotropic He-Ne laser in axial magnetic field

G.L. Kononchuk, S.M. Yegorov*

Taras Shevchenko Kyiv Univ., 6 Glushkova Prosp., 252127 Kyiv, Ukraine

Tel. 8 044 261 36 77, E-mail: lukich@optics.ups.kiev.ua

* Tel. 8 044 443 02 93, E-mail: sequenser@mail.ru

Abstract. On the basis of the general Lamb model the set of six coupled nonlinear differential equations has been derived for two-mode $\lambda = 0.63$ mm laser operation with the presence both amplitude and phase anisotropy and axial magnetic field. Numeric integration of the set of equations and the Lyapunov stability analysis have been proceeded. It turned out that in zero magnetic field in the presence of the amplitude anisotropy both stable time-independent states with parallelly or orthogonally polarized modes and non-stationary state are possible. Changing orientation and nonorthogonality/nonparallelity of polarization planes in magnetic field are considered. Influence of mode-mode interaction is discussed.

Keywords: anisotropy, He-Ne laser, magnetic field, polarization instability.

Paper received 28.05.99; revised manuscript received 08.07.99; accepted for publication 12.07.99.

1. Introduction

The roots of a quasi-isotropic He-Ne laser have been set up in the paper of Sargent et al. [1] where the general equations for intensities and frequencies for an arbitrary atomic transition, any number of excited longitudinal modes and in the presence of magnetic field of arbitrary direction have been derived. But influence of a cavity anisotropy was not described consistently. Another theory has been developed in the paper of Lenstra [2]. In this work influence of different cavity anisotropy types on behaviour of polarization characteristics was considered in general for an arbitrary atomic transition of laser having been placed in axial or transversal magnetic field.

Single-mode laser operating was considered on the basis of the papers [1,2] for a wide range of atomic transitions and laser parameters (see, for example, [2,3] and references therein). For two-mode operation such detailed analysis has not yet been given. In the paper of Lenstra [2] qualitative remarks were made about behaviour of a $j=1 \Rightarrow j=2$ transition laser without magnetic field and in the case of weak linear phase or amplitude anisotropy. The investigation of Svirina et al. [3] is restricted to the case of a phase cavity anisotropy of a $j=1 \Rightarrow j=2$ ($\lambda=0.63$ μm) laser in axial magnetic field.

In the present paper we have derived, within the framework of the general Lamb model, the two-mode operation

equations with the presence both amplitude and phase anisotropy and axial magnetic field. Each spatial mode is described as a sum of two ones polarized right- and left-circularly. So, we get the set of six coupled nonlinear differential equations for four intensities of polarization modes and two phase angles of spatial modes. Numeric solution is carried out by the Runge-Kutta routine for the $j=1 \Rightarrow j=2$ transition and with only amplitude anisotropy being presented. The time-independent solutions with different polarization states we had got were tested with respect to stability by the Lyapunov analysis, and then a conclusion about existence of stationary states has been made.

2. Intensity-and phase-determining equations

The present paper is based upon the formalism brought forward by Sargent et al. [1]. In accordance to it, a laser field is a sum of cavity eigenstates, and the active medium polarization is calculated by the density matrix routine up to the third terms by the electromagnetic field. Each longitudinal mode is described as a sum of two ones polarized right- and left-circularly. There are two equations for each circular mode: for its intensity and for its phase. So, there are $4n$ equations in the full equation set, where n is the number of longitudinal modes. However, because of all right parts of the equations include a *phase difference* (so called phase angle) but not phases separately, we can replace two sepa-

rate equations for phases with one for a phase angle. This is correct if we consider only time-independent solutions. Hence, the full set includes $3n$ equations.

In the case of two longitudinal laser modes we have the following intensity- and phase-determining equations:

$$\begin{aligned} \frac{\dot{I}_{1+}}{I_{1+}} = & \alpha_{1+} - \beta_{1+}I_{1+} - \theta_{1\pm}I_{1-} - \theta_{1+2+}I_{2+} - \theta_{1+2-}I_{2-} - \theta'_{1+} \sqrt{\frac{I_{1-}}{I_{1+}}} \sqrt{I_{2+}I_{2-}} \times \\ & \times \cos(\psi_1 - \psi_2) - \tau'_{1+} \sqrt{\frac{I_{1-}}{I_{1+}}} \sqrt{I_{2+}I_{2-}} \sin(\psi_1 - \psi_2) - \sqrt{\frac{I_{1-}}{I_{1+}}} (Q_{xy} \cos \psi_1 - \tilde{v}_{xy} \sin \psi_1) \end{aligned} \quad (1)$$

$$\begin{aligned} \frac{\dot{I}_{1-}}{I_{1-}} = & \alpha_{1-} - \beta_{1-}I_{1-} - \theta_{1\mp}I_{1+} - \theta_{1-2+}I_{2+} - \theta_{1-2-}I_{2-} - \theta'_{1-} \sqrt{\frac{I_{1+}}{I_{1-}}} \sqrt{I_{2+}I_{2-}} \times \\ & \times \cos(\psi_1 - \psi_2) + \tau'_{1-} \sqrt{\frac{I_{1+}}{I_{1-}}} \sqrt{I_{2+}I_{2-}} \sin(\psi_1 - \psi_2) - \sqrt{\frac{I_{1+}}{I_{1-}}} (Q_{xy} \cos \psi_1 + \tilde{v}_{xy} \sin \psi_1) \end{aligned} \quad (2)$$

$$\begin{aligned} \frac{\dot{I}_{2+}}{I_{2+}} = & \alpha_{2+} - \beta_{2+}I_{2+} - \theta_{2\pm}I_{2-} - \theta_{2+1+}I_{1+} - \theta_{2+1-}I_{1-} - \theta'_{2+} \sqrt{\frac{I_{2-}}{I_{2+}}} \sqrt{I_{1+}I_{1-}} \times \\ & \times \cos(\psi_2 - \psi_1) - \tau'_{2+} \sqrt{\frac{I_{2-}}{I_{2+}}} \sqrt{I_{1+}I_{1-}} \sin(\psi_2 - \psi_1) - \sqrt{\frac{I_{2-}}{I_{2+}}} (Q_{xy} \cos \psi_2 - \tilde{v}_{xy} \sin \psi_2) \end{aligned} \quad (3)$$

$$\begin{aligned} \frac{\dot{I}_{2-}}{I_{2-}} = & \alpha_{2-} - \beta_{2-}I_{2-} - \theta_{2-1+}I_{2+} - \theta_{2-1+}I_{1+} - \theta_{2-1-}I_{1-} - \theta'_{2-} \sqrt{\frac{I_{2+}}{I_{2-}}} \sqrt{I_{1+}I_{1-}} \times \\ & \times \cos(\psi_2 - \psi_1) + \tau'_{2-} \sqrt{\frac{I_{2+}}{I_{2-}}} \sqrt{I_{1+}I_{1-}} \sin(\psi_2 - \psi_1) - \sqrt{\frac{I_{2+}}{I_{2-}}} (Q_{xy} \cos \psi_2 + \tilde{v}_{xy} \sin \psi_2) \end{aligned} \quad (4)$$

$$\begin{aligned} \dot{\psi}_1 = & \sigma_{1+} - \sigma_{1-} - (\rho_{1+} - \tau_{1\mp})I_{1+} - (\tau_{1\pm} - \rho_{1-})I_{1-} - (\tau_{1+2+} - \tau_{1-2+})I_{2+} - (\tau_{1+2-} - \tau_{1-2-})I_{2-} - (\tau'_{1+} - \tau'_{1-}) \sqrt{I_{2+}I_{2-}} \times \\ & \times \cos(\psi_1 - \psi_2) + (\theta'_{1+} + \theta'_{1-}) \sqrt{I_{2+}I_{2-}} \sin(\psi_1 - \psi_2) + Q_{xy} \sin \psi_1 \left(\sqrt{\frac{I_{1+}}{I_{1-}}} + \sqrt{\frac{I_{1-}}{I_{1+}}} \right) + \tilde{v}_{xy} \cos \psi_1 \left(\sqrt{\frac{I_{1+}}{I_{1-}}} - \sqrt{\frac{I_{1-}}{I_{1+}}} \right) \end{aligned} \quad (5)$$

$$\begin{aligned} \dot{\psi}_2 = & \sigma_{2+} - \sigma_{2-} - (\rho_{2+} - \tau_{2\mp})I_{2+} - (\tau_{2\pm} - \rho_{2-})I_{2-} - (\tau_{2+1+} - \tau_{2-1+})I_{1+} - (\tau_{2+1-} - \tau_{2-1-})I_{1-} - (\tau'_{2+} - \tau'_{2-}) \sqrt{I_{1+}I_{1-}} \times \\ & \times \cos(\psi_2 - \psi_1) + (\theta'_{2+} + \theta'_{2-}) \sqrt{I_{1+}I_{1-}} \sin(\psi_2 - \psi_1) + Q_{xy} \sin \psi_2 \left(\sqrt{\frac{I_{2+}}{I_{2-}}} + \sqrt{\frac{I_{2-}}{I_{2+}}} \right) + \tilde{v}_{xy} \cos \psi_2 \left(\sqrt{\frac{I_{2+}}{I_{2-}}} - \sqrt{\frac{I_{2-}}{I_{2+}}} \right) \end{aligned} \quad (6)$$

where I_{n+} , I_{n-} are the intensities of the right- and left-handed circular waves of the n -th spatial mode, ψ_n is its phase angle, $Q_{xy} = (c/4L)(l_x - l_y)$ is the amplitude cavity anisotropy and $\tilde{v}_{xy} = (c/4L)(\phi_x - \phi_y)$ is the phase one, c is the light velocity, L is the cavity length, l_x and l_y are losses, and ϕ_x and ϕ_y are phase changes for the waves polarized in x - and y -direction. α , β , θ , θ' , σ , ρ , τ , τ' are calculated from the density matrix motion equation. These calculations and used assumptions are adduced in the Appendix. Let's note that in amplitude equations an appropriate α coefficient is responsible for a mode gain while β and θ 's are the self-saturation and cross-saturation parameters, and in the phase equations σ , ρ , τ coefficients are responsible for the mode frequency pulling/pushing phenomena (change of the op-

eration frequency to or from the centre of the gain line with respect to the eigenfrequency of an empty cavity). These coefficients have their analogues in single-mode equations. But θ' , τ' don't have. We can say that they are responsible for some sort of gain saturation and frequency change as

well but those ones depend besides on mode-mode phase relations.

2. Time-independent solutions

A) Zero magnetic field

Numeric integration of the set of equations (1)-(6) was performed for the $j=1 \Rightarrow j=2$ ($\lambda = 0.63 \mu\text{m}$) transition and following parameters: the Lorentz width $\gamma_{ab} = 225$ MHz, the upper and the lower atomic levels width $\gamma_a = 160$ MHz and $\gamma_b = 290$ MHz, the gain $\eta = 1.33 \dots 1.38$, the Doppler parameter $Ku = 1010$ MHz, the spatial mode interval $D = \nu_2 - \nu_1 = 640$ MHz and several values of the amplitude anisotropy

Q_{xy} . It turned out that at weak anisotropy the state with modes polarized linearly in orthogonal planes is stable on the most part of the gain profile while the nearest to the centre mode is polarized in the lower loss plane. Hence, each mode being moved through the gain profile undergoes two changes of a polarization plane. This is outlined in the Fig.1. When a mode is in a hatched area it is polarized in the lower loss plane. That is conventionally signed with a horizontal arrow in the figure. At the same time the another mode is in a clear area and has the orthogonal polarization signed with a vertical arrow. Frequencies $\omega_0 \pm D/2$ correspond to the symmetric location of the modes with respect to the centre of transition line. It is just this point that has the unstable range where none of solutions is stable. Those are the dotted areas in the Fig.1. When anisotropy being risen from 0 to certain value the instability range spreads on full duty cycle. This value is about 10 kHz for the given set of parameters. The biggest Lyapunov exponents determining whether a stable solution exists are shown in the Fig.2 for some anisotropy values. The mentioned phenomenon evidently follows from mode-mode interaction. It is absent at single-mode operation when at any value of amplitude anisotropy there is a stable solution with mode polarization in the lower loss plane.

When anisotropy being further risen (up to about 100 kHz for the used set of parameters), the state with both modes

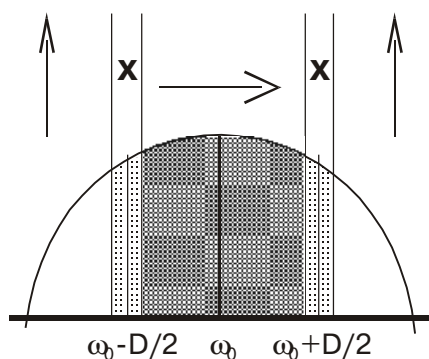


Fig. 1. Direction of mode polarization plane versus its location at the gain line at weak anisotropy.

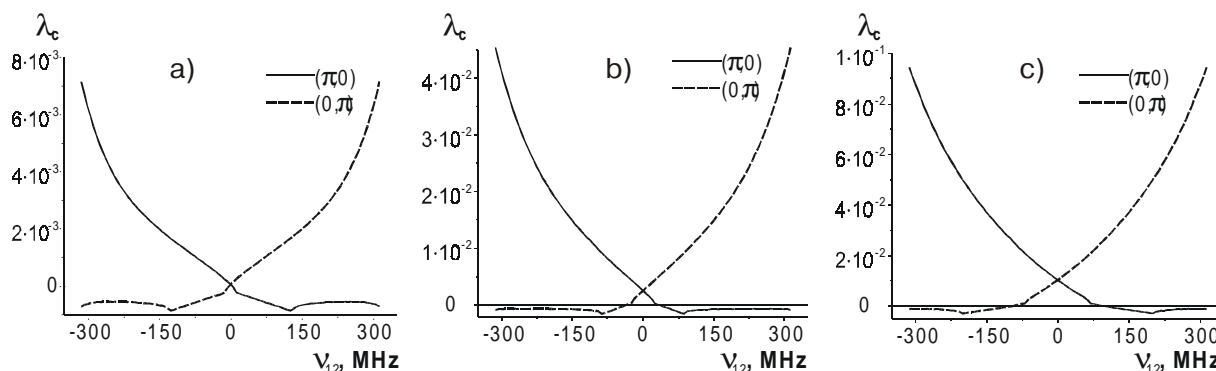


Fig. 2. The determinative Lyapunov exponent versus the middle intermode frequency, $(\nu_2 + \nu_1)/2$ at $\gamma_{ab} = 225$ MHz, $\gamma_a = 160$ MHz, $\gamma_b = 290$ MHz, $\eta = 1.33$, $Ku = 1010$ MHz, $D = 640$ MHz and $Q_{xy} = 0.5$ kHz (a), $Q_{xy} = 3.0$ kHz (b), $Q_{xy} = 6.0$ kHz (c) without applied magnetic field.

polarized in the lower loss plane becomes stable on full duty cycle. Such situation is realized in a commercial laser LGN-207B with Brewster's window introducing considerable amplitude anisotropy into a cavity.

B) Nonzero magnetic field

In studying a laser in external magnetic field we were mainly interested in two questions: 1) do linear polarization planes remain orthogonal, and 2) how does magnetic field change their orientation.

The set of equations (1)-(6) has been integrated for two values of the cavity anisotropy: $5 \cdot 10^{-4}$ MHz and $1 \cdot 10^{-1}$ MHz at different magnitudes of external magnetic field. It follows from preceding consideration that in zero field at $Q_{xy} = 5 \cdot 10^{-4}$ MHz the state with modes polarized linearly in orthogonal planes is stable on almost full gain profile while an instability range is very narrow, it is less than 6 MHz. At $Q_{xy} = 5 \cdot 10^{-4}$ MHz the state with both modes polarized in the lower loss plane is stable on full duty cycle.

First of all, it is worth noting that a spatial mode always has nonzero ellipticity in magnetic field owing to nonequality of left- and right-circularly polarized modes intensities. So, we will mean a direction of the bigger axis of a polarization ellipse as a direction of a polarization vector.

Calculated angles of the modes polarization planes and the interplane angle versus the middle intermode frequency $\nu_{12} = (\nu_1 + \nu_2)/2$ (where ν_1 and ν_2 are modes operation frequencies) are shown in the Figs 3,4. The mode being called the first has the lower frequency while the mode being called the second has the higher one with respect to each other. It is worth noting that the interplane angle is close enough but not equal to that without field (i.e. to 0° or 90°) on the full duty cycle except the central tuning of one mode (when its frequency is close to the central transition frequency) at both values of anisotropy. At the central tuning the interplanes angle equals to that without field to within calculation errors. The polarization planes undergo turn in magnetic field. The fact is that the stronger anisotropy a cavity has the higher field magnitude is needed for that turn to be significant. In both considered cases the turn is more significant at the close to symmetrical tuning while it is small at the close to central tuning contrary to single-mode operation when turn of the polarization plane of a mode is greater at the central

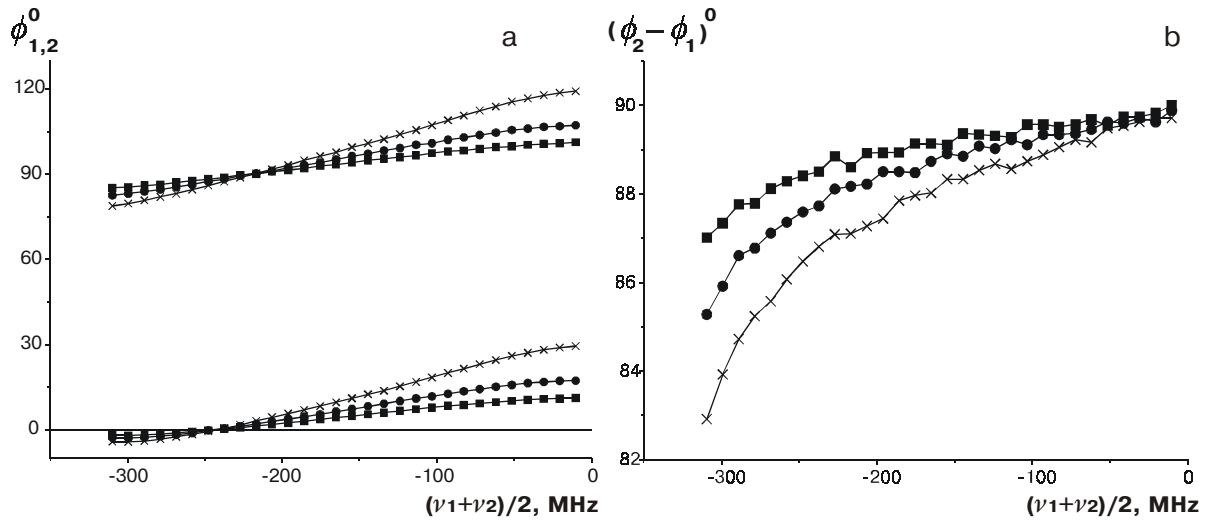


Fig. 3. Calculated angles of the modes polarization planes ϕ_1, ϕ_2 (a) and the interplane angle $\phi_2 - \phi_1$ (b) versus the middle intermode frequency, $(\nu_2 + \nu_1)/2$. The squared line corresponds to magnetic field $H = 0.2\text{G}$, the circled line – to $H = 0.3\text{G}$, the crossed line – to $H = 0.45\text{G}$. $Q_{xy} = 0.5$ kHz, the other parameters are the same as in Fig.2.

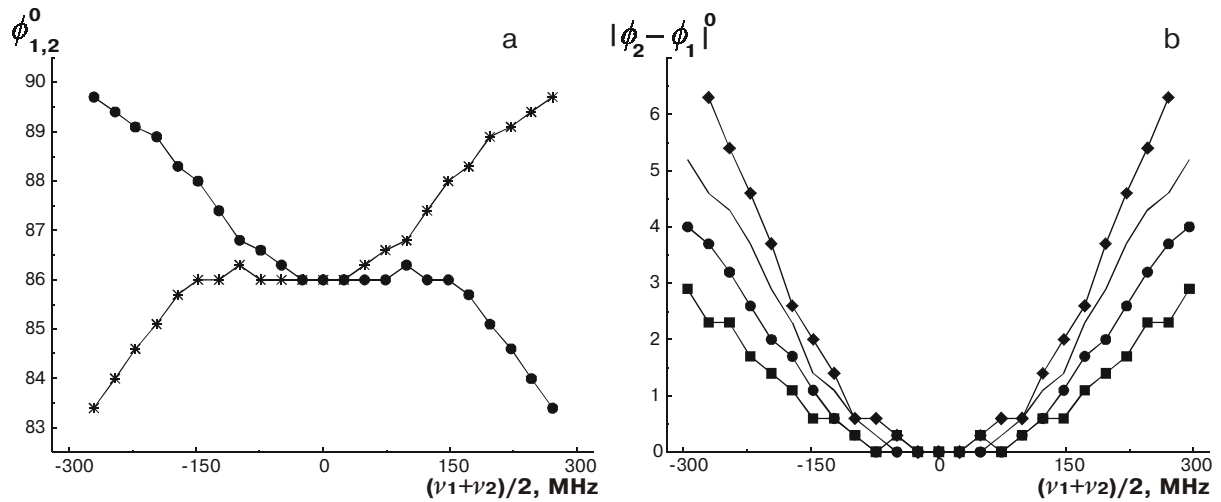


Fig. 4. Calculated angles of the modes polarization planes ϕ_1, ϕ_2 (a) and the module of the interplane angle $|\phi_2 - \phi_1|$ (b) versus the middle intermode frequency, $(\nu_2 + \nu_1)/2$. $H = 20\text{G}$ and the circled line corresponds to mode 1 and the crossed – to mode 2 in (a). The squared line corresponds to $H = 8\text{G}$, the circled line – to $H = 12\text{G}$, the plane line – to $H = 16\text{G}$, the diamonded line – to $H = 20\text{G}$. $Q_{xy} = 100$ kHz, $\eta = 1.38$, and the other parameters are the same as in Fig.2.

tuning. We can conclude that the mentioned phenomenon is a result of coupled action of the external magnetic field and mode-mode interaction. That is a reflection of a new type items in the set of equations which are absent in single-mode operation equations.

Conclusions

In the present paper a two-mode $\lambda = 0.63 \mu\text{m}$ laser operation with the presence both amplitude and phase anisotropy and axial magnetic field was considered on the basis of the general Lamb model. Numeric integration of the nonlinear equations set gave a number of time-independent solutions,

and the Lyapunov stability analysis have been proceeded for them. It was found that without magnetic field at weak anisotropy the state with linearly polarized in orthogonal planes modes is stable at almost full duty cycle with the nearest to the centre mode is polarized in the lower loss plane while at strong enough anisotropy the state with both modes polarized in the lower loss plane becomes stable on full duty cycle. It turned out that even in zero magnetic field no time-independent state exists at the close to the symmetrical tuning in the presence of weak amplitude anisotropy. The interplane angle and angles of the modes polarization planes was enumerated in nonzero field. It was found that changing orientation and nonorthogonality/nonparallelity of the polarization planes takes place. They

are more significant at the close to symmetrical tuning contrary to single-mode operation when the turn of the polarization plane of a mode is greater at the central tuning. It was concluded that the reported phenomena belongs to the mode-mode interaction depending on the mode-mode phase correlations between them.

Appendix

$\alpha, \beta, \theta, \theta', \sigma, \rho, \tau, \tau'$ can be evaluated on the basis of the paper [1]. In the present paper these values have been calculated in assumption of lifetimes equality of both atomic levels magnetic sublevels involved and equality of the Lande factors of both atomic levels involved, one isotope, no nuclear spin and active medium filling all the cavity. σ is the real part while α is the imaginary one of the complex coefficient \mathbf{A} ,

$$\alpha_{n\pm} = \text{Im}(\mathbf{A}_{n\pm}), \quad \sigma_{n\pm} = \text{Re}(\mathbf{A}_{n\pm}), \quad (\text{A.1})$$

where

$$\mathbf{A}_{n\pm} = (v\epsilon_0\hbar^3/8Ku) \times \sum_{a,b} \delta_{a',b'\pm 1} (\mathcal{D}_{a',b'})^2 (\eta Z[\gamma_{ab} + i(\pm\mu_B gH - v_{\pm})] - 1), \quad (\text{A.2})$$

$n = 1, 2$, v is the operating frequency of the given mode, $v_{n\pm}$ is the *detuning* of the mode from the atomic line centre, g is the factor Lande, H is the magnitude of external magnetic field, \mathcal{D}_{ab} is an electric dipole matrix element, Ku is the Doppler parameter, γ_{ab} is the Lorentz width, η is the mode gain, $Z[x]$ is the plasma integral.

Coefficients ρ, τ, τ' are real parts while β, θ, θ' are imaginary ones of complex Θ 's.

$$\begin{aligned} \beta_{n\pm} &= \text{Im}(\Theta_{n\pm, n\pm}), & \theta_{n\pm} &= \text{Im}(\Theta_{n\pm}), \\ \theta_{n\pm, n'\mp} &= \text{Im}(\Theta_{n\pm, n'\mp}), & \theta'_{n\pm} &= \text{Im}(\Theta'_{n\pm}), \end{aligned} \quad (\text{A.3a})$$

$$\begin{aligned} \rho_{n\pm} &= \text{Re}(\Theta_{n\pm, n\pm}), & \tau_{n\pm} &= \text{Re}(\Theta_{n\pm}), \\ \tau_{n\pm, n'\mp} &= \text{Re}(\Theta_{n\pm, n'\mp}), & \tau'_{n\pm} &= \text{Re}(\Theta'_{n\pm}), \end{aligned} \quad (\text{A.3b})$$

For different Θ 's we have:

$$\Theta_{n\pm, n\pm} = (\eta v \epsilon_0 \hbar^3 / 8Ku) \sum_{a,b} \delta_{a', b' \pm 1} (\mathcal{D}_{a', b'})^4 \sum_{t=1}^4 T_{t1}(v_{tk}), \quad (\text{A.4})$$

where $n=1, 2$, the $T_{t1}(v_{tk})$ are in the Doppler limit as follows:

$$T_{t1} = 2i\sqrt{\pi} [v_{t2}(v_{t1} + v_{t3})]^{-1}, \quad T_{t2} \approx 0, \quad T_{t3} \approx 0, \quad (\text{A.5})$$

the arguments v_{tk} can be found in the table A.1.

$$\begin{aligned} \Theta_{n\pm, n'\pm} &= (\eta v \epsilon_0 \hbar^3 / 8Ku) \sum_{a,b} \delta_{a', b' \pm 1} (\mathcal{D}_{a', b'})^4 \times \\ &\times \left\{ \sum_{t=1}^4 T_{t1}(v_{tk}) + \sum_{t=1}^4 T_{t1}(v_{tk}) \right\} \end{aligned} \quad (\text{A.6})$$

where $n, n' = 1, 2$; $n \neq n'$ (if $n = n'$ the former equation should be used). Let's note two sums of the $T_{tk}(v_{tk})$ functions in the

Table A.1. This table defines the arguments of T_{t1} appearing in the third-order integrals $\Theta_{n\pm, n\pm}$ (A.4)

	$k=1$	$k=2$	$k=3$
$t=1$	$\gamma_{ab} + i(\pm\mu_B gH - v_{n\pm})$	γ^a	$\gamma_{ab} + i(\mp\mu_B gH - v_{n\pm})$
$t=2$	$\gamma_{ab} + i(\pm\mu_B gH - v_{n\pm})$	γ^a	$\gamma_{ab} + i(\mp\mu_B gH - v_{n\pm})$
$t=3$	$\gamma_{ab} + i(\pm\mu_B gH - v_{n\pm})$	γ^b	$\gamma_{ab} + i(\mp\mu_B gH + v_{n\pm})$
$t=4$	$\gamma_{ab} + i(\pm\mu_B gH - v_{n\pm})$	γ^b	$\gamma_{ab} + i(\mp\mu_B gH - v_{n\pm})$

Table A.2. This table defines the arguments of T_{t1} appearing in the third-order integrals $\mathbf{Q}_{n\pm, n\pm}$ (A.6)

$\Sigma^{(1)}$	$k=1$	$k=2$	$k=3$
$t=1$	$\gamma_{ab} + i(\pm\mu_B gH - v_{n\pm})$	γ^a	$\gamma_{ab} + i(\mp\mu_B gH - v_{n\pm})$
$t=2$	$\gamma_{ab} + i(\pm\mu_B gH - v_{n\pm})$	γ^a	$\gamma_{ab} + i(\mp\mu_B gH + v_{n\pm})$
$t=3$	$\gamma_{ab} + i(\pm\mu_B gH - v_{n\pm})$	$\gamma^b + i(v_{n'} \pm - v_{n\pm})$	$\gamma_{ab} + i(\mp\mu_B gH + v_{n\pm})$
$t=4$	$\gamma_{ab} + i(\pm\mu_B gH - v_{n\pm})$	$\gamma^b + i(v_{n'} \pm - v_{n\pm})$	$\gamma_{ab} + i(\mp\mu_B gH - v_{n\pm})$
$\Sigma^{(2)}$	$k=1$	$k=2$	$k=3$
$t=1$	$\gamma_{ab} + i(\pm\mu_B gH - v_{n\pm})$	$\gamma^a + i(v_{n'} \pm - v_{n\pm})$	$\gamma_{ab} + i(\pm\mu_B gH - v_{n\pm})$
$t=2$	$\gamma_{ab} + i(\pm\mu_B gH - v_{n\pm})$	$\gamma^a + i(v_{n'} \pm - v_{n\pm})$	$\gamma_{ab} + i(\mp\mu_B gH + v_{n\pm})$
$t=3$	$\gamma_{ab} + i(\pm\mu_B gH - v_{n\pm})$	γ^b	$\gamma_{ab} + i(\mp\mu_B gH + v_{n\pm})$
$t=4$	$\gamma_{ab} + i(\pm\mu_B gH - v_{n\pm})$	γ^b	$\gamma_{ab} + i(\mp\mu_B gH - v_{n\pm})$

Table A.3. This table defines the arguments of T_{t1} appearing in the third-order integrals $Q_{n\pm, n' \mp}$ (A.7)

$\Sigma^1)$	$k=1$	$k=2$	$k=3$
$t=1$	$\gamma_{ab+i(\pm\mu BgH-vn\pm)}$	γ^a	$\gamma_{ab+i(\mp\mu BgH-vn\pm)}$
$t=2$	$\gamma_{ab+i(\pm\mu BgH-vn\pm)}$	γ^a	$\gamma_{ab+i(\pm\mu BgH+vn\pm)}$
$t=3$	$\gamma_{ab+i(\pm\mu BgH-vn\pm)}$	$\gamma_{b+i(\pm 2\mu BgH+vn' \mp -vn\pm)}$	$\gamma_{ab+i(\pm\mu BgH+vn\pm)}$
$t=4$	$\gamma_{ab+i(\pm\mu BgH-vn\pm)}$	$\gamma_{b+i(\pm 2\mu BgH+vn' \mp -vn\pm)}$	$\gamma_{ab+i(\pm\mu BgH-vn\pm)}$
$\Sigma^2)$	$k=1$	$k=2$	$k=3$
$t=1$	$\gamma_{ab+i(\pm\mu BgH-vn\pm)}$	$\gamma_{a+i(\pm 2\mu BgH+vn' \mp -vn\pm)}$	$\gamma_{ab+i(\pm\mu BgH-vn\pm)}$
$t=2$	$\gamma_{ab+i(\pm\mu BgH-vn\pm)}$	$\gamma_{a+i(\pm 2\mu BgH+vn' \mp -vn\pm)}$	$\gamma_{ab+i(\pm\mu BgH+vn\pm)}$
$t=3$	$\gamma_{ab+i(\pm\mu BgH-vn\pm)}$	γ^b	$\gamma_{ab+i(\pm\mu BgH+vn\pm)}$
$t=4$	$\gamma_{ab+i(\pm\mu BgH-vn\pm)}$	γ^b	$\gamma_{ab+i(\pm\mu BgH+vn\pm)}$

Table A.4. This table defines the arguments of T_{t1} appearing in the third-order integrals $Q'_{n\pm}$ (A.8)

$\Sigma^1)$	$k=1$	$k=2$	$k=3$
$t=1$	$\gamma_{ab+i(\pm\mu BgH-vn \mp +vn' \mp -vn\pm)}$	$\gamma_{a+i(vn' \mp -vn\pm)}$	$\gamma_{ab+i(\mp\mu BgH-vn\pm)}$
$t=2$	$\gamma_{ab+i(\pm\mu BgH-vn \mp +vn' \mp -vn\pm)}$	$\gamma_{a+i(vn' \mp -vn\pm)}$	$\gamma_{ab+i(\pm\mu BgH+vn\pm)}$
$t=3$	$\gamma_{ab+i(\pm\mu BgH-vn \mp +vn' \mp -vn\pm)}$	$\gamma_{b+i(\pm 2\mu BgH+vn' \mp -vn\pm)}$	$\gamma_{ab+i(\pm\mu BgH+vn\pm)}$
$t=4$	$\gamma_{ab+i(\pm\mu BgH-vn \mp +vn' \mp -vn\pm)}$	$\gamma_{b+i(\pm 2\mu BgH+vn' \mp -vn\pm)}$	$\gamma_{ab+i(\pm\mu BgH-vn\pm)}$
$\Sigma^2)$	$k=1$	$k=2$	$k=3$
$t=1$	$\gamma_{ab+i(\pm\mu BgH-vn \mp +vn' \mp -vn\pm)}$	$\gamma_{a+i(\pm 2\mu BgH+vn' \mp -vn\pm)}$	$\gamma_{ab+i(\pm\mu BgH-vn\pm)}$
$t=2$	$\gamma_{ab+i(\pm\mu BgH-vn \mp +vn' \mp -vn\pm)}$	$\gamma_{a+i(\pm 2\mu BgH+vn' \mp -vn\pm)}$	$\gamma_{ab+i(\pm\mu BgH+vn\pm)}$
$t=3$	$\gamma_{ab+i(\pm\mu BgH-vn \mp +vn' \mp -vn\pm)}$	$\gamma_{b+i(vn' \mp -vn\pm)}$	$\gamma_{ab+i(\pm\mu BgH+vn\pm)}$
$t=4$	$\gamma_{ab+i(\pm\mu BgH-vn \mp +vn' \mp -vn\pm)}$	$\gamma_{b+i(vn' \mp -vn\pm)}$	$\gamma_{ab+i(\mp\mu BgH-vn\pm)}$

brackets. This is reflected in the following table A.2 which consists of two parts for the first and for the second sum.

$$\Theta_{n\pm, n' \mp} = (\eta v \epsilon_0 \hbar^3 / 8Ku) \sum_{a,b} \delta_{a', b \pm 1} \{ (\mathcal{P}_{a', b'})^2 (\mathcal{P}_{a', b \pm 2})^2 \times \sum_{t=1}^4 {}^1 T_{t1}(v_{tk}) + (\mathcal{P}_{a', b'})^2 (\mathcal{P}_{a', b \mp 2})^2 \sum_{t=1}^4 {}^2 T_{t1}(v_{tk}) \} \quad (A.7)$$

where $n, n' = 1, 2$, the arguments v_{tk} are in the table A.3.

$$\Theta'_{n\pm} = (\eta v \epsilon_0 \hbar^3 / 8Ku) \sum_{a,b} \delta_{a', b \pm 1} \{ (\mathcal{P}_{a', b'})^2 (\mathcal{P}_{a', b \pm 2})^2 \times$$

$$\times \sum_{t=1}^4 {}^1 T_{t1}(v_{tk}) + (\mathcal{P}_{a', b'})^2 (\mathcal{P}_{a', b \mp 2})^2 \sum_{t=1}^4 {}^2 T_{t1}(v_{tk}) \} \quad (A.8)$$

where $n = 1, 2$, the arguments v_{tk} are in the table A.4.

References

1. M. Sargent III, W. E. Lamb, R. L. Fork, Theory of a Zeeman Laser I, II // *Phys. Rev.* **164**(2), pp.436-465 (1964)
2. D. Lenstra, On the theory of polarization effects in gas laser // *Phys. Reports* **59**(3), pp.301-373 (1980)
3. L. P. Svirina, Polarization instability in a two-frequency gas laser with a weakly anisotropical cavity // *Optika i spektroskopiya* **77**(1), pp.124-133 (1994) (in Russian).